Electrochemistry Communications 12 (2010) 1792–1795

Contents lists available at ScienceDirect

Electrochemistry Communications

journal homepage: www.elsevier.com/locate/elecom

Cyanamide-derived non-precious metal catalyst for oxygen reduction

Hoon T. Chung [a], Christina M. Johnston [a], Kateryna Artyushkova [b], Magali Ferrandon [c], Deborah J. Myers [c], Piotr Zelenay [a,*]

[a] Materials Physics and Applications Division, Los Alamos National Laboratory Los Alamos, NM 87545, USA
[b] Department of Chemical and Nuclear Engineering, University of New Mexico Albuquerque, NM 87131, USA
[c] Chemical Sciences and Engineering Division, Argonne National Laboratory Argonne, IL 60439, USA

ARTICLE INFO

Article history:
Received 6 October 2010
Accepted 22 October 2010
Available online 29 October 2010

Keywords:
Polymer electrolyte fuel cell
Oxygen reduction reaction
Non-precious metal catalyst

ABSTRACT

Cyanamide was used in the preparation series of metal–nitrogen–carbon (M–N–C) oxygen reduction catalysts. The best catalyst, treated at 1050 °C, shows good performance versus previously reported non-precious metal catalysts with an OCV ~1.0 V and a current density of 105 mA/cm^2 (*iR*-corrected) at 0.80 V in H_2/O_2 fuel cell testing (catalyst loading: 4 mg cm^{-2}). Although nitrogen content has been previously correlated positively with ORR activity, no such trend is observed here for any nitrogen type. The combined effects of nitrogen and sulfur incorporation into the carbon may account for the high activity of the 1050 °C catalyst.

© 2010 Elsevier B.V. All rights reserved.

1. Introduction

To date, the only catalysts that can succeed under the demanding polymer electrolyte fuel cell (PEFC) conditions of relatively low temperature (80 °C) and high acidity are based on platinum. Transition metal–nitrogen–carbon (M–N–C) catalysts are considered to be the best non-precious candidate materials for substituting platinum in PEFCs, especially after recent advances in activity and durability [1]. Following early work with unpyrolyzed Me–N_4 macrocycles [2], the introduction of a heat-treatment step [3] and the use of simpler precursors [4,5] have contributed greatly to enhancing the catalytic activity and durability of this class of catalysts. Several studies have reported the effect of nitrogen source on the catalytic activity, with certain precursors like ethylene diamine (EDA) [6] and nitroaniline [7] demonstrating higher activities.

In the research discussed herein, cyanamide was selected as the nitrogen precursor, capable of forming graphitic-C_3N_4 under certain pyrolysis conditions [8]. Graphitic-C_3N_4 (g-C_3N_4) has a high nitrogen content, which is often associated with ORR activity in non-precious metal catalysts [5,6]. Though we intended to increase the nitrogen content in the graphene carbon structure by adding cyanamide, this was not the outcome. Instead, cyanamide aided the incorporation of sulfur from the iron sulfate precursor into the carbon. In this report we discuss our observations concerning the effect of heat-treatment temperature on nitrogen content, sulfur content, and ORR catalytic activity.

2. Experimental

The catalysts were synthesized by mixing 2.0 g cyanamide (CM) and 1.5 g $FeSO_4 \cdot 7H_2O$ (or 1.1 g $Fe(CH_3COO)_2$) with 1.0 g oxidized carbon (Ketjenblack EC-300J = KB), pretreated in 70% nitric acid at 80 °C for 8 h. After mixing, two heat-treatment steps followed at 800–1050 °C in nitrogen atmosphere. The temperature of both heat-treatment steps was kept the same, so a single heat-treatment temperature is referred to in the text for each sample. Between heat-treatments, the catalyst was leached in 0.5 M H_2SO_4 at 80 °C for 8 h in order to remove acid-soluble components.

The cathode catalyst ink for the membrane-electrode assembly (MEA) was prepared by ultrasonically blending the catalyst with de-ionized water and recast Nafion® ionomer (5% Nafion® in alcohol; Solution Technology, Inc). The catalyst:water:ionomer weight ratios were *ca.*1:20:0.6. The catalyst ink was hand-brushed onto the membrane (Nafion®117) and gas diffusion layer (GDL, E-TEK). 0.25 mg cm^{-2} Pt (catalyzed cloth GDL, E-TEK) was used as the anode. MEAs were hot-pressed at 120 °C for 90 s. A 5-cm^2 cell was used for fuel cell testing.

X-ray photoelectron spectroscopy (XPS) measurements were performed on a Kratos Axis Ultra spectrometer using a Mg Kα X-ray source. A Dycor Dymaxion quadrupole mass spectrometer was used for the mass analyses. The product gas concentration of the samples heated from room temperature to 1050 °C at a rate of 5 °C/min in Ar at a flow rate of 25 mL/min was analyzed for masses up to 100. Thermogravimetric analysis (TGA) to determine Fe content was performed using a TA Q50 instrument.

3. Results and discussion

Fig. 1a, b and c displays the results of H_2–O_2 fuel cell tests of the CM-derived catalysts prepared with different iron sources ($FeSO_4 \cdot$

* Corresponding author. Tel.: +1 505 667 0197; fax: +1 505 665 4292.
E-mail address: zelenay@lanl.gov (P. Zelenay).

1388-2481/$ – see front matter © 2010 Elsevier B.V. All rights reserved.
doi:10.1016/j.elecom.2010.10.027

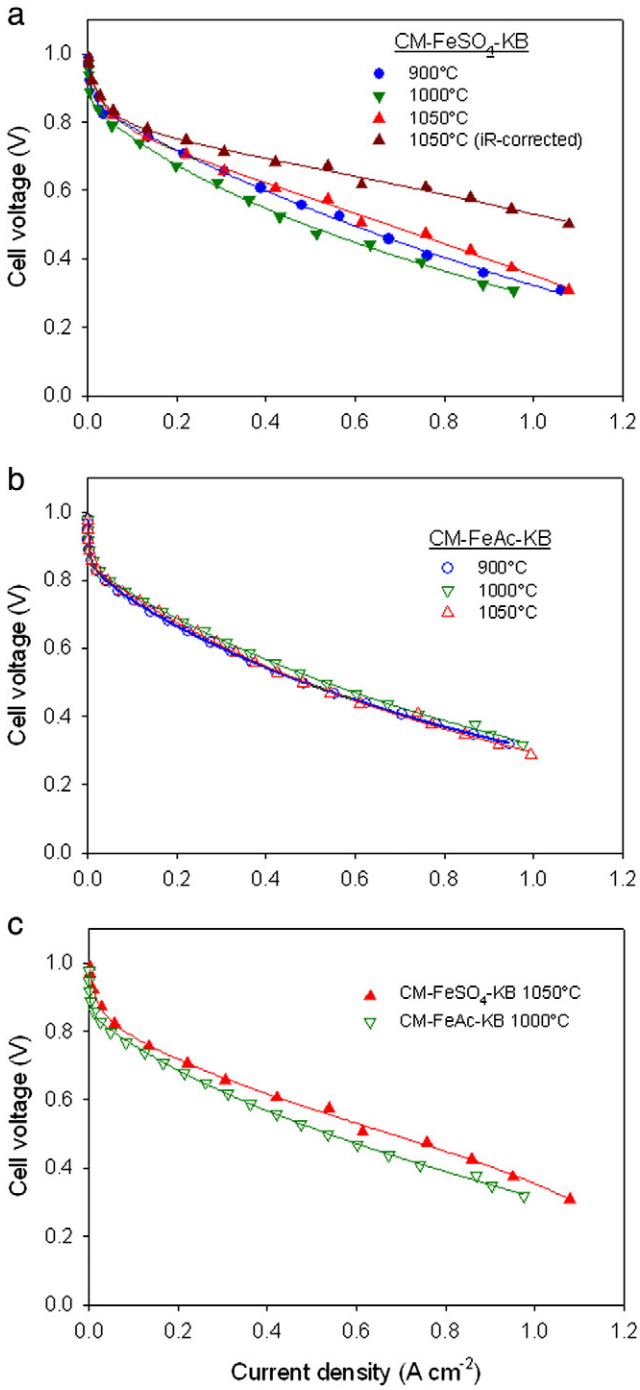

Fig. 1. (a) Fuel cell polarization plots recorded with CM–$FeSO_4$–KB ORR catalysts obtained at different heat-treatment temperatures. (b) Fuel cell polarization plots recorded with CM–FeAc–KB ORR catalysts obtained at different heat-treatment temperatures. (c) Fuel cell polarization plots comparison with CM–$FeSO_4$–KB heat-treated at 1050 °C and CM–FeAc–KB heat-treated at 1000 °C. Nafion®117 membrane; anode — 30 psig H_2, 0.25 mg cm^{-2} Pt (catalyzed-cloth GDL, E-TEK); cathode — 30 psig O_2, non-precious catalyst loading 4.0 mg cm^{-2} (double-sided cloth GDL, E-TEK); humidification for H_2 and O_2 was 100% RH; constant 300/500 standard mL per minute anode/cathode flow rates for H_2 and O_2 respectively; MEA surface area 5 cm^2.

$7H_2O$ and $Fe(CH_3COO)_2$ = FeAc). For the CM–$FeSO_4$–KB 900 °C and 1050 °C heat-treated catalysts, the OCV is ~1.0 V in both cases and the current densities are 70 mA and 83 mA (105 mA for *iR*-corrected) at 0.80 V, respectively. Based on these values, the CM-derived catalysts compare favorably to the top five most active non-precious metal catalysts recently reviewed [1]. Improvement in catalyst performance is observed up to a heat-treatment temperature of 900 °C [9], but the performance decreases when the catalyst is pyrolyzed at 1000 °C. Interestingly, the highest performance is attained when the heat-treatment temperature is further increased to 1050 °C. (This property is also observed when using Black Pearls 2000 as the carbon support; data not shown). The pattern differs from the CM–FeAc–KB catalysts (Fig. 1b) and the majority of M–N–C catalyst reports that show a volcano-type plot of activity versus pyrolysis temperature [4,10]. Such behavior should relate to the identity of the active site(s).

According to previous reports, the nitrogen content and type present in M–N–C catalysts is important for ORR activity [5,6,11,12]. As depicted in Fig. 2a, there are several types of nitrogen species that can be largely classified as "two-p-electron donors" and "one-p-electron donors" to the π band of carbon. The two-p-electron donor species (especially graphitic and pyrrolic-N) are expected to lower the carbon band gap energy and possibly promote catalytic activity [13]. The one-p-electron donor, pyridinic-N, also has a lone pair of electrons available for binding with metal atoms (see Fig. 2a); indeed, pyridinic nitrogen content has been the most closely correlated to the activities of M–N–C catalysts [5,6,11,12].

Using these categories to label the nitrogen, the XPS peak at 398.8 eV (pyridinic-N) was assigned as "one e^- donor", and the XPS peaks appearing at 400.2 eV (pyrrolic-N) and 401.4 eV (graphitic-N) were labeled as "two e^- donor" to construct the plot in Fig. 2b [14]. Clearly, the total nitrogen content (from 2.2 to 0.9 at%), the one-e^--

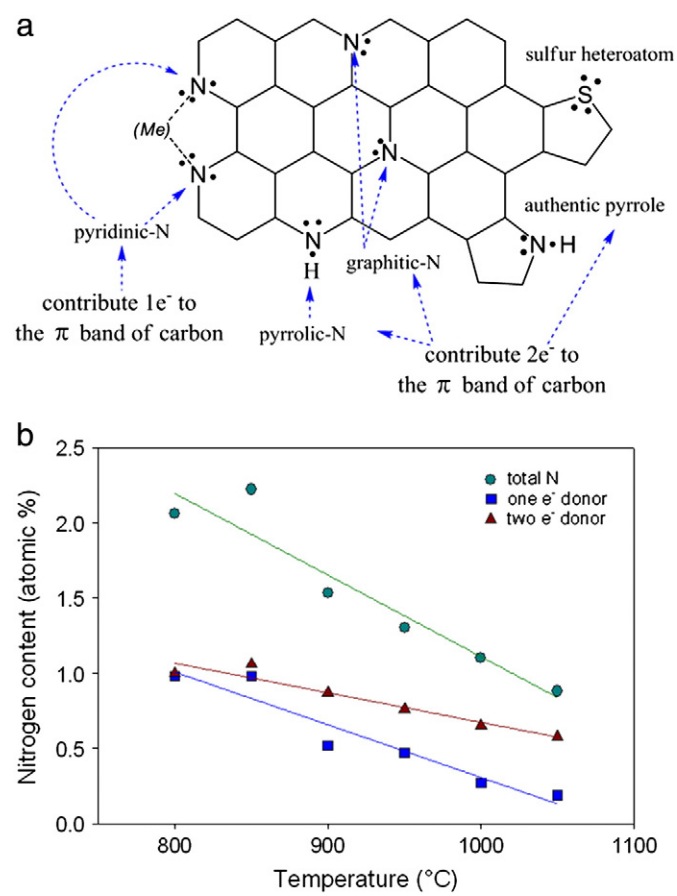

Fig. 2. (a) A schematic diagram of pyridinic, pyrrolic, graphitic, and authentic pyrrole nitrogen and thiophene sulfur content incorporated into the graphene carbon layer. The labels for nitrogen types are those commonly used in literature [5,15]. (b) One-e^- donor-type, two-e^- donor-type, and total nitrogen content variation with heat-treatment temperature as determined by N 1 s XPS. One-e^- donor-type nitrogen content was determined from B.E. 398.8 eV, and two e^- donor-type nitrogen content from B.E. 400.2 and 401.4 eV. Total nitrogen content is the sum of the two types.

donor, and the two-e$^-$-donor nitrogen content all decrease monotonically with increasing pyrolysis temperature. These downward trends do not match the unusual pattern of the ORR activity results discussed earlier. (Note that using other definitions of nitrogen type does not reveal any correlating pattern.) Therefore, other factors must be considered to explain the higher activity and usual activity pattern of CM–$FeSO_4$–KB catalysts.

The Fe content of the CM–$FeSO_4$–KB catalysts was determined by TGA to be 11–14 wt% (after the 2nd heat treatment), and the Fe content of the CM–FeAc–KB catalysts was shown to be about half at 6 wt%. These values are quite high compared to other non-precious catalysts [1], and imply the presence of excess, inactive Fe forms. Notably, the $FeSO_4$-derived catalysts retain more Fe than those prepared from FeAc, in contrast to a previous report that noted the beneficial role of sulfur in the removal of inactive Fe species [15].

The CM–$FeSO_4$–KB-based catalyst discussed herein contains sulfur due to the iron source, ferrous sulfate 7-hydrate ($FeSO_4 \cdot 7H_2O$). Fig. 3a shows S_{2p} spectra of 1050 °C heat-treated catalysts; the other catalysts show a similar pattern. The first two peaks (162.3 eV and 163.4 eV) and second two peaks (164.4 eV and 165.7 eV) are doublet structures due to spin-orbit coupling ($S_{2p3/2}$ and $S_{2p1/2}$). The peak at 164.4 eV has been attributed previously to $S_{2p3/2}$ of thiophene [15,16], and the peak at 162.3 eV has been assigned before to $S_{2p3/2}$ of thiolate [16] or thiocyanate [15]. Comparing the intensities of both peaks, sulfur is found to exist mainly as thiophene, as depicted in Fig. 3a. The total and thiophene-type sulfur content in the catalyst increases with temperature, as shown in Fig. 3b. In a previous report, sulfur in sulfate form did not react with carbon to form C-heteroatoms [15], in contrast to these results. Fig. 3c shows the evolution of SO_2 (mass 64), as detected by mass spectrometry during the first heat treatment of samples composed of $FeSO_4 \cdot 7H_2O$ mixed with Ketjenblack EC-300J, both with and without the addition of cyanamide. With cyanamide, the decomposition of the sulfate and evolution of SO_2 is greatly depressed, indicating that an interaction between cyanamide and sulfate (or sulfate-derived species) stabilizes sulfur in the sample perhaps through the formation of C–S bonds. The details of this mechanism are being investigated.

To further determine whether sulfur enhances the ORR activity of the CM-based catalyst, samples were prepared using iron(II) acetate as the iron source rather than iron sulfate, thus avoiding any sulfur addition. The performance of these catalysts at high voltage/low current density (under kinetic rather than mass-transport control) is half that of the catalyst prepared from the iron sulfate precursor, as shown in Fig. 1c. This difference strongly indicates that sulfur is responsible for the improved activity of CM-based catalysts.

The effect of sulfur on the ORR catalytic activity has been rarely studied [15,17]. As shown in Fig. 2a, however, sulfur has the potential to enhance ORR activity in the same manner as "one-e$^-$-donor" and "two-e$^-$-donor" nitrogens. Sulfur resembles the "one-e$^-$-donor" nitrogen in having a lone pair of electrons, which can possibly interact with metal atoms [5]. It also resembles "two-e$^-$-donor" nitrogen by having two p electrons that can interact with the π band of the graphene layer. Consequently, the high ORR activity in spite of a decreasing amount of nitrogen of all types and unusual activity dependence on temperature in CM–$FeSO_4$–KB could possibly be explained by the beneficial effect of sulfur incorporation. Alternate explanations for these results involve indirect effects of sulfur on carbon structure. For example, it was recently reported that the addition of sulfur results in extended graphene layers and smaller graphitic domain size [15], which should affect the carbon electronic structure [15]. Direct electronic effects of sulfur (i.e., sulfur incorporation) were also suggested in that prior report, but no correlation between sulfur content and ORR activity could be demonstrated because only a single sample type was examined [15]. In future work, we will attempt to discriminate between the indirect structural and direct electronic effects of sulfur. Because the sulfur content at 1050 °C is comparable to that of nitrogen (0.6 at.% versus 0.9 at.%), the direct effect of sulfur heteroatoms on the carbon electronic structure could be significant.

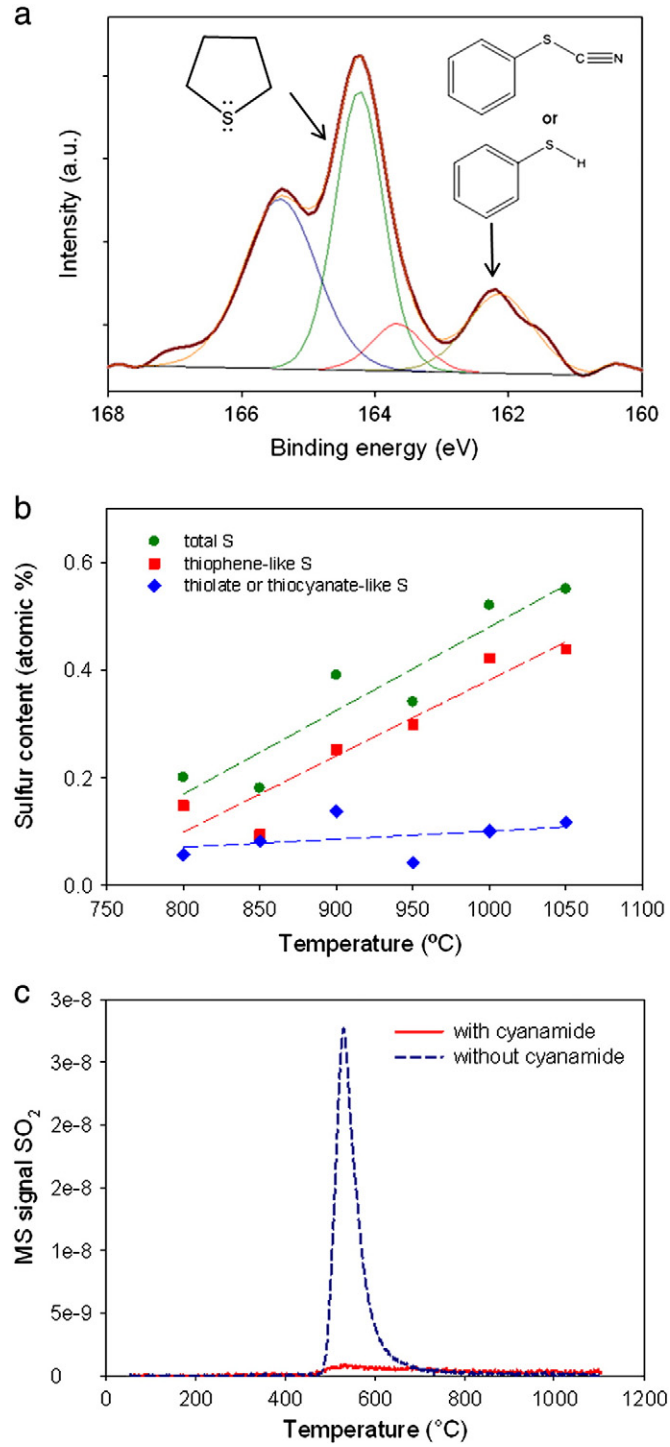

Fig. 3. (a) XPS S_{2p} spectra of the pyrolyzed cyanamide-derived catalyst at 1050 °C. (b) Total, thiophene-like and thiolate (or thiocyanide)-like sulfur content variation with temperature as determined by XPS. (c) Ionic current of the mass spectroscopy of SO_2 of $FeSO_4 \cdot 7H_2O$-Ketjenblack samples obtained with and without the addition of cyanamide; (m/e = 64 SO_2).

4. Conclusion

Cyanamide used as a nitrogen source for an M–N–C type catalyst was found to generate catalysts with high ORR activity, as well as a

distinctive, non-monotonic activity dependence on heat-treatment temperature. The best performing catalyst, obtained via a heat treatment at 1050 °C catalyst, yielded an OCV of ~1.0 V and current density of 105 mA/cm^2 at 0.80 V (*iR*-corrected). Cyanamide was found to suppress sulfur evolution as SO_2 from the iron source, ferrous sulfate 7-hydrate ($FeSO_4 \cdot 7H_2O$), during heat-treatment, resulting in the incorporation of sulfur into the catalyst. The sulfur content increased with heat-treatment temperature. The high activity and unique pattern of ORR activity with pyrolysis temperature may relate to the combination of nitrogen and sulfur effects.

Acknowledgements

Financial support of the DOE-EERE Fuel Cell Technologies Program as well as Los Alamos National Laboratory through the Laboratory-Directed Research and Development program (LDRD) is gratefully acknowledged.

References

[1] F. Jaouen, J. Herranz, M. Lefèvre, J.-P. Dodelet, U. Kramm, I. Herrmann, P. Bogdanoff, J. Maruyama, T. Nagaoka, A. Garsuch, J.R. Dahn, T. Olson, S. Pylypenko, P. Atanassov, E.A. Ustinov, Appl. Mater. Interfaces 8 (2009) 1623.
[2] R. Jasinski, Nature 201 (1964) 1212.
[3] H. Jahnke, M. Schönborn, G. Zimmermann, Top. Curr. Chem. 61 (1976) 133.
[4] S. Gupta, D. Tryk, I. Bae, W. Aldred, E.B. Yeager, J. Appl. Electrochem. 19 (1989) 19.
[5] G. Faubert, R. Côtè, J.-P. Dodelet, M. Lefèvre, P. Bertrand, Electrochim. Acta 44 (1999) 2589.
[6] V. Nallathambi, J.W. Lee, S.P. Kumaraguru, G. Wu, B.N. Popov, J. Power Sources 183 (2008) 34.
[7] T.E. Wood, Z. Tan, A.K. Schmoeckel, D. O'Neill, R. Atanasoski, J. Power Sources 178 (2008) 510.
[8] M. Groenewolt, M. Antonietti, Adv. Mater. 17 (2005) 1789.
[9] H.T. Chung, C.M. Johnston, P. Zelenay, ECS Trans. 25 (1) (2009) 485.
[10] M. Lefèvre, J.P. Dodelet, P. Bertrand, J. Phys. Chem. B 106 (2002) 8705.
[11] P.H. Matter, U.S. Ozkan, Catal. Lett. 109 (2006) 115.
[12] S. Maldonado, K.J. Stevenson, J. Phys. Chem. B 109 (2005) 4707.
[13] V.V. Strelko, V.S. Kuts, P.A. Thrower, Carbon 38 (2000) 1499.
[14] J.R. Pels, F. Kapteijn, J.A. Moulijn, Q. Zhu, K.M. Thomas, Carbon 33 (1995) 1641.
[15] I. Hermann, U.I. Kramm, J. Radnik, S. Fiechter, P. Bogdanoff, J. Electrochem. Soc. 156 (2009) B1283.
[16] F. Buckel, F. Effenberger, C. Yan, A. Gölzhäuser, M. Grunze, Adv. Mater. 12 (2000) 901.
[17] E.J. Biddinger, D.S. Knapke, D. von Deak, U.S. Ozkan, Appl. Catal. B 96 (2010) 72.